

*Supporting Information*

**Chiral Detection by Induced Surface-Enhanced Raman Optical Activity**

**Moumita Das, Debraj Gangopadhyay, Jaroslav Šebestík, Lucie Habartová, Pavel Michal,  
Josef Kapitán, and Petr Bouř**

**Contents**

[Figure S1.](#) SEROA and SERS spectra for eight linker and chiral acid combinations.

[Table S1.](#) Vibrational band positions and assignment of the main linker bands.

[Figure S2.](#) SERS spectra of L-tartaric acid.

[Table S2.](#) CID ratios for Selected Bands.

[Figure S3.](#) Time dependence of the SEROA and SERS spectra.

[Figure S4.](#) Absorption spectra, example.

[Figure S5.](#) Circular dichroism spectra.

[Figure S6.](#) Calculated Raman and ROA spectra model clusters.

[Figure S7.](#) Calculated CD and absorption spectra of the clusters.

[Figure S8.](#) CD and absorption spectra of the first model calculated at three approximation levels.

[Table S3.](#) Cluster 2, selected transitions within 520-540 nm.

[Figure S9.](#) Model geometries.

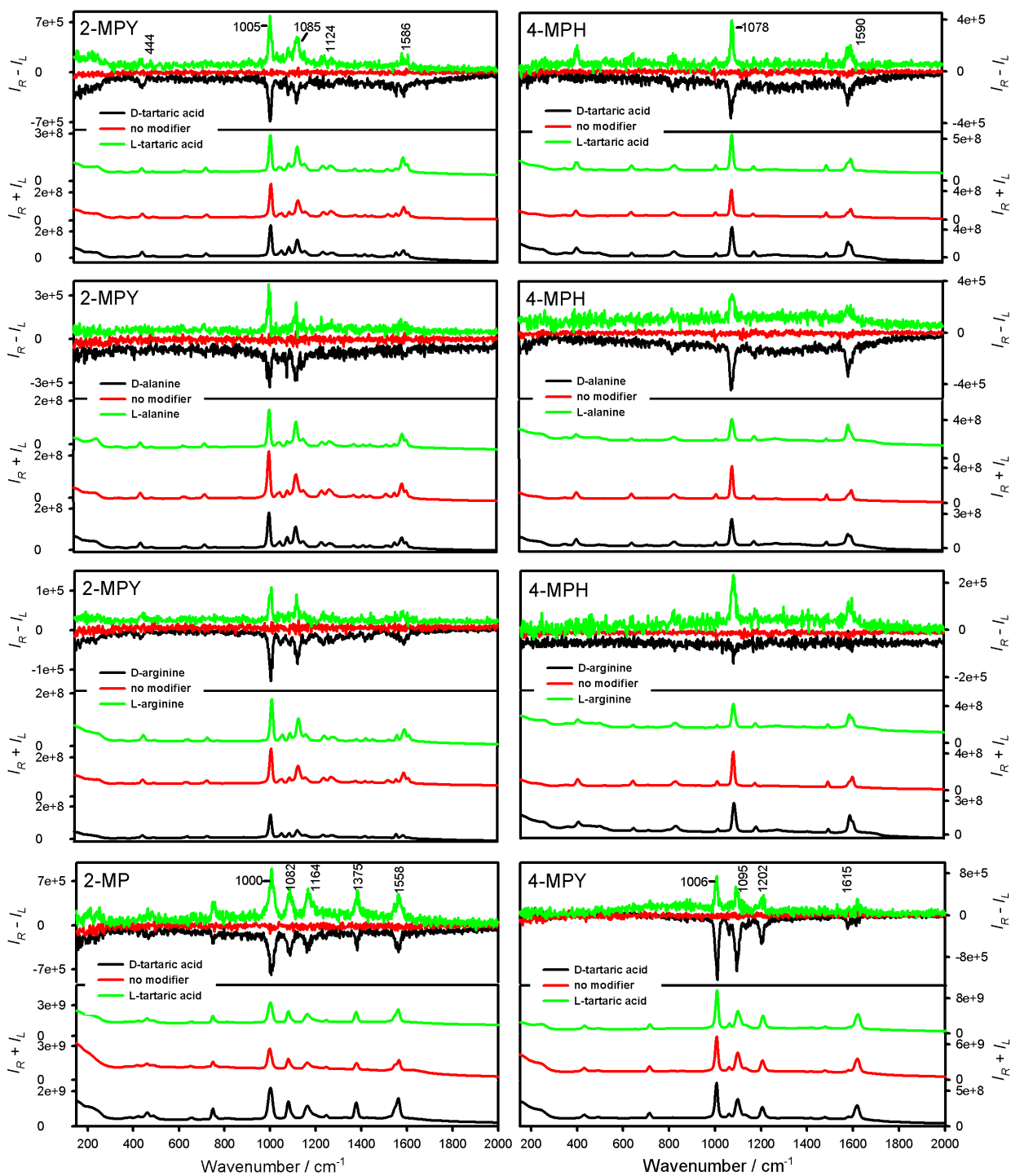
[Experimental details](#)

[Preparation of Silver Nanoparticles](#)

[SERS and ROA Spectra](#)

[CD and UV-vis Absorption](#)

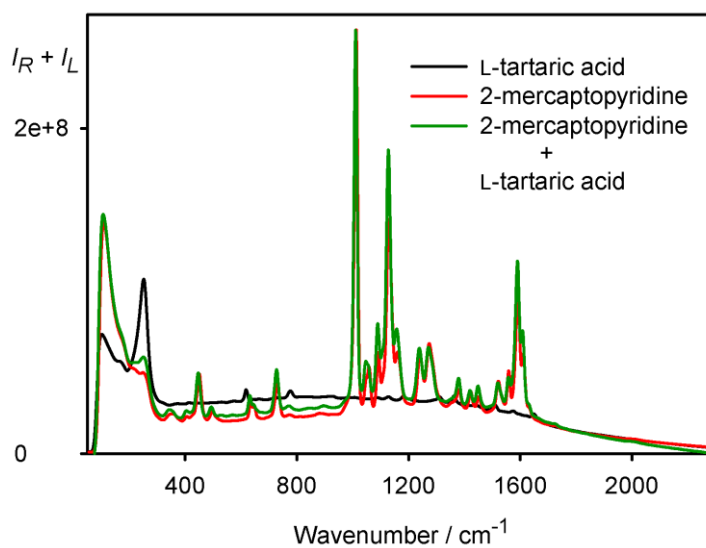
[Computations](#)



**Figure S1.** SEROA and SERS spectra for eight linker and chiral acid combinations; SERS spectra are arbitrarily y-shifted for better visibility.

**Table S1.** Vibrational band positions and assignment of the main linker bands.<sup>1</sup>

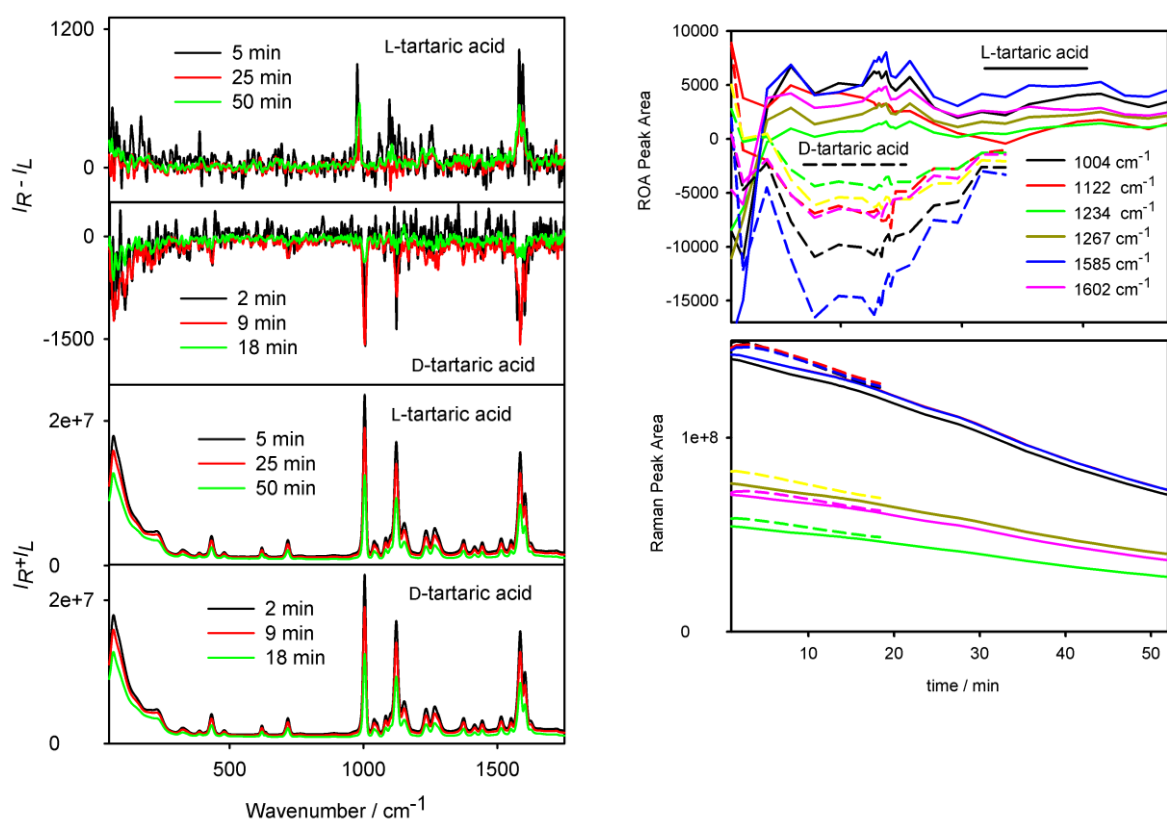
	Position (cm <sup>-1</sup> )	Vibration
<b>2-MPY:</b>	444	out of plane bending,
	1005	ring breathing
	1085	in plane CH bending
	1124	in plane CH bending
	1586	CC, CN stretching
<b>4-MPH:</b>	1078	ring breathing
	1590	CC stretching
<b>4-MPY:</b>	1006	ring breathing
	1095	in plane CH bending
	1202	in plane CN, CC, CH bending
	1615	CC stretching
<b>2-MP:</b>	1000	ring breathing
	1082	in plane CH bending
	1164	in plane CH bending
	1375	CC stretching
	1558	CN stretching



**Figure S2.** SERS spectra of L-tartaric acid (100 mM), 2-mercaptopyridine, and a combination.

**Table S2.** CID ratios for Selected Bands

	Position/cm <sup>-1</sup>	L-tar	D-tar	L -ala	D -ala	L -arg	D -arg
<b>2-MPY</b>	1005	1.3×10 <sup>-3</sup>	-2.4×10 <sup>-3</sup>	1.9×10 <sup>-3</sup>	-1.5×10 <sup>-3</sup>	6×10 <sup>-4</sup>	-8.5×10 <sup>-4</sup>
	1124	1.9×10 <sup>-3</sup>	-2.98×10 <sup>-3</sup>	2.0×10 <sup>-3</sup>	-2.2×10 <sup>-3</sup>	1.3×10 <sup>-3</sup>	-1.7×10 <sup>-3</sup>
<b>4-MPH</b>	1078	8.1×10 <sup>-4</sup>	-6.7×10 <sup>-4</sup>	8.9×10 <sup>-4</sup>	-1.4×10 <sup>-3</sup>	7.9×10 <sup>-4</sup>	-3.4×10 <sup>-4</sup>
	1590	1.1×10 <sup>-3</sup>	-9.9×10 <sup>-4</sup>	6.6×10 <sup>-4</sup>	-2.5×10 <sup>-3</sup>	7.8×10 <sup>-4</sup>	-2.8×10 <sup>-4</sup>
<b>4-MPY</b>	1006	1.1×10 <sup>-4</sup>	-1.4×10 <sup>-4</sup>	-	-	-	-
	1095	1.7×10 <sup>-4</sup>	-1.8×10 <sup>-4</sup>	-	-	-	-
	1202	1.8×10 <sup>-4</sup>	-1.4×10 <sup>-4</sup>	-	-	-	-
<b>2-MP</b>	1000	2.2×10 <sup>-4</sup>	-1.8×10 <sup>-4</sup>	-	-	-	-
	1082	2.3×10 <sup>-4</sup>	-1.8×10 <sup>-4</sup>	-	-	-	-
	1164	2.8×10 <sup>-4</sup>	-2.1×10 <sup>-4</sup>	-	-	-	-
	1375	2.3×10 <sup>-4</sup>	-1.6×10 <sup>-4</sup>	-	-	-	-
	1558	1.7×10 <sup>-4</sup>	-1.7×10 <sup>-4</sup>	-	-	-	-

**Figure S3.** Time dependence of SEROA and SERS spectra of 2-mercaptopyridine with tartaric acid, and integrated intensities of selected Raman and ROA bands (for the Palacký University spectrometer).

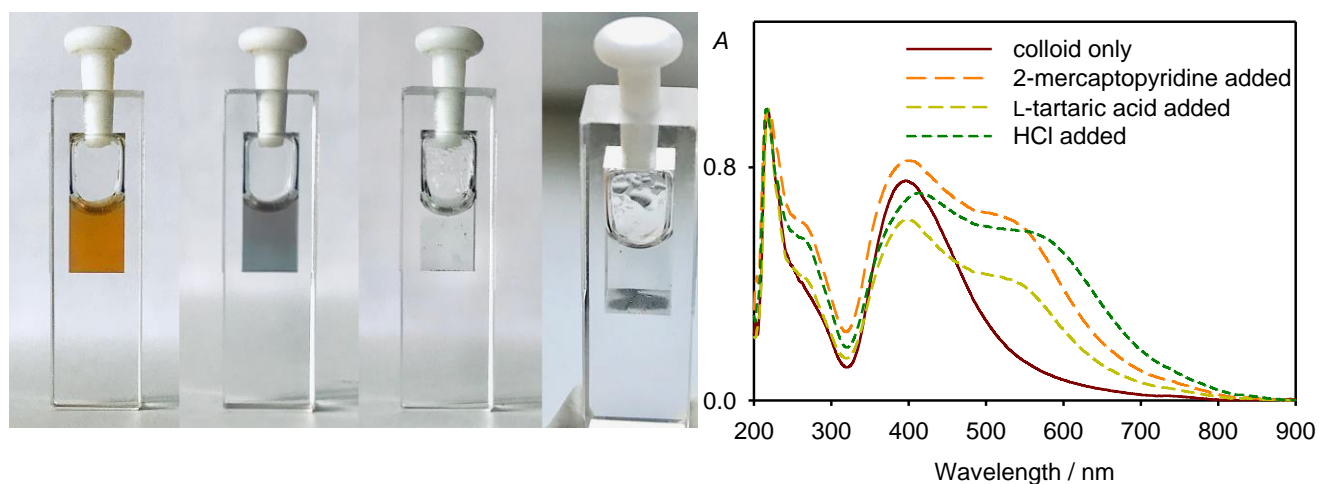


**Figure S4.** Left: colloid solution before measurement (orange), after the aggregation was triggered by HCl (grey), and final state (last two, transparent, silver precipitated at the bottom). Right: absorption spectra for an experiment with 2-mercaptopyridine and L-tartaric acid.

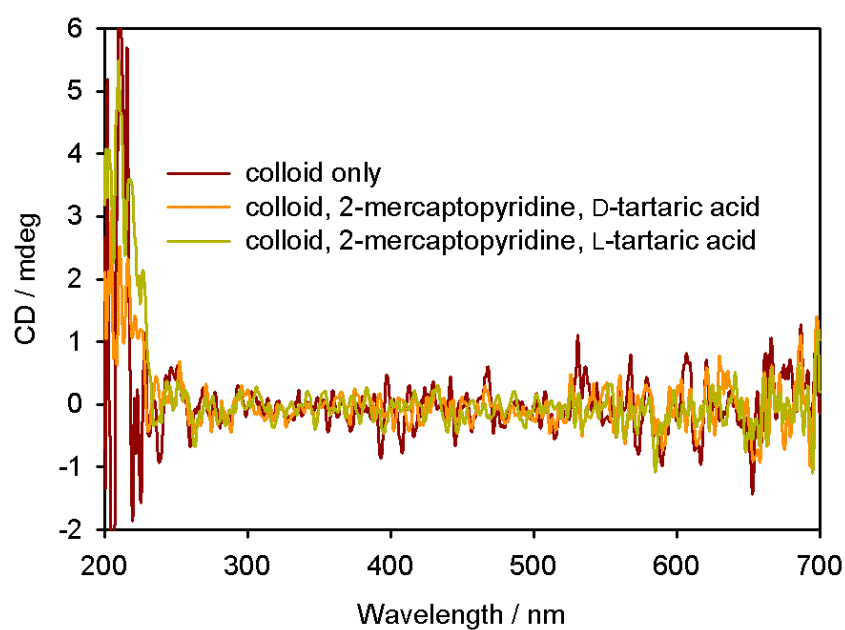


**Figure S5.** Circular dichroism spectra of the 2-mercaptopyridine/tartaric acid experiments.

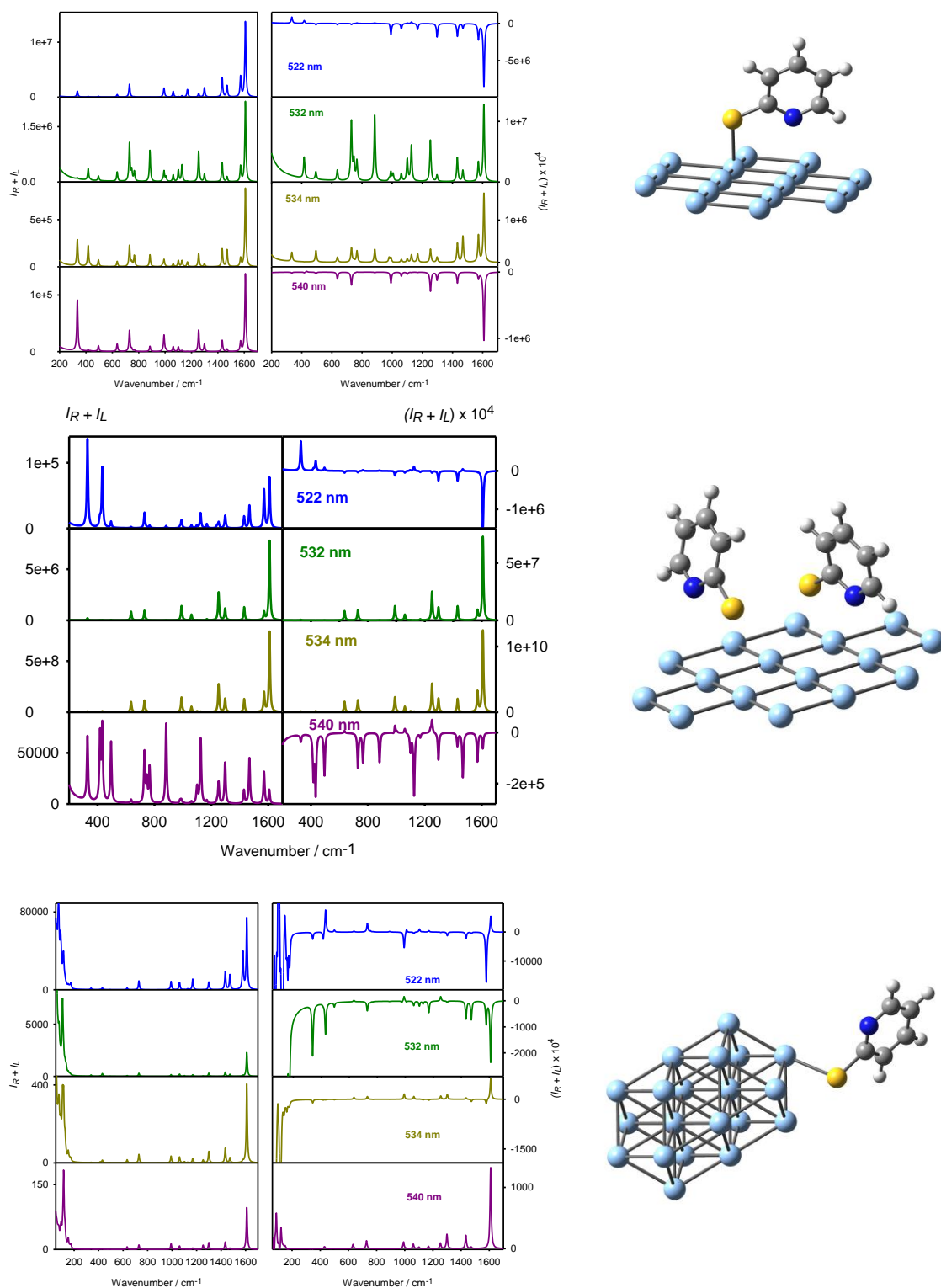


**Figure S6.** Raman and ROA spectra of three 2-mercaptopyridine/silver clusters calculated for four excitation wavelengths.

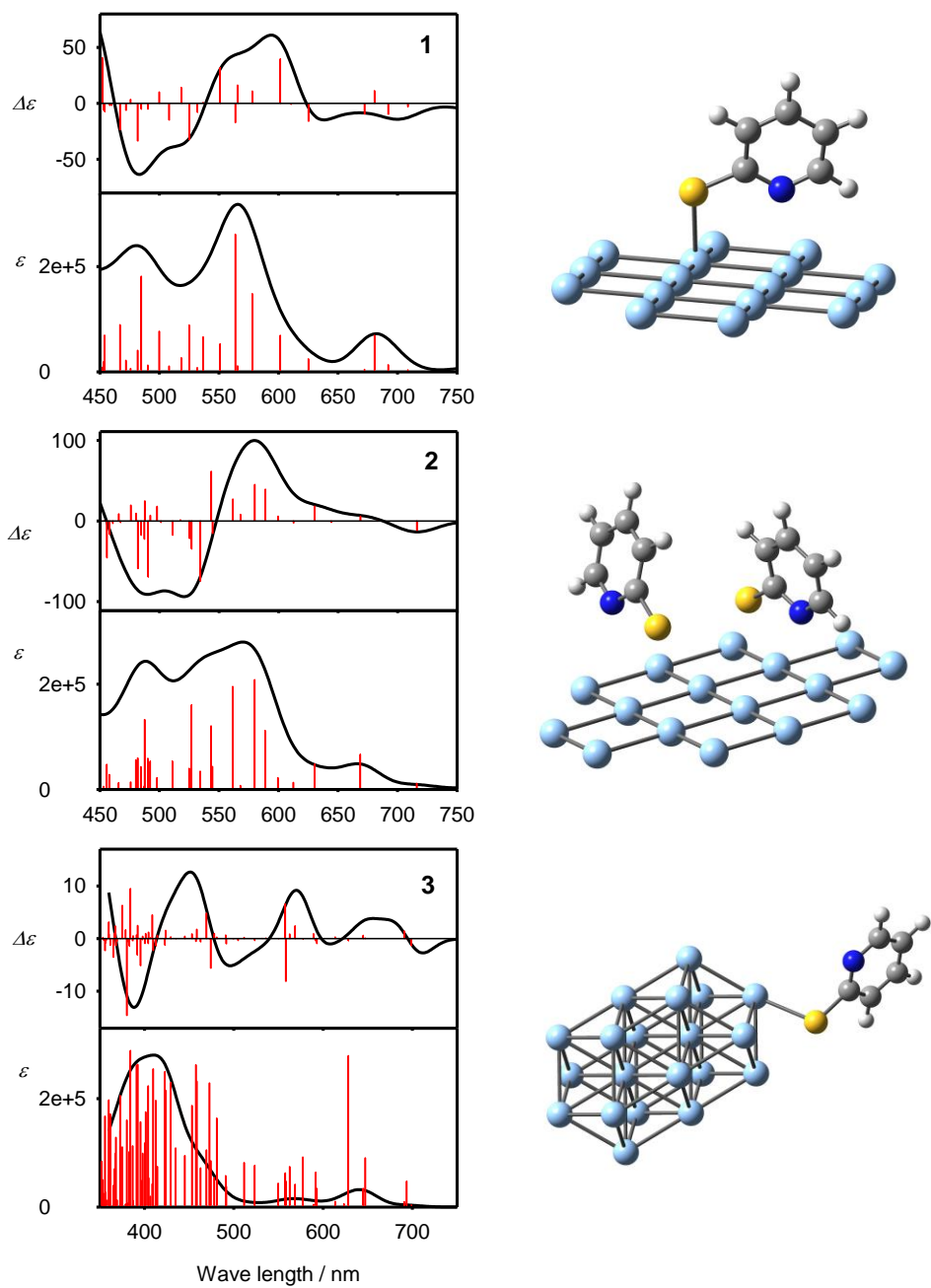


**Figure S7.** Calculated CD and absorption spectra of the three 2-MPY/Ag clusters.

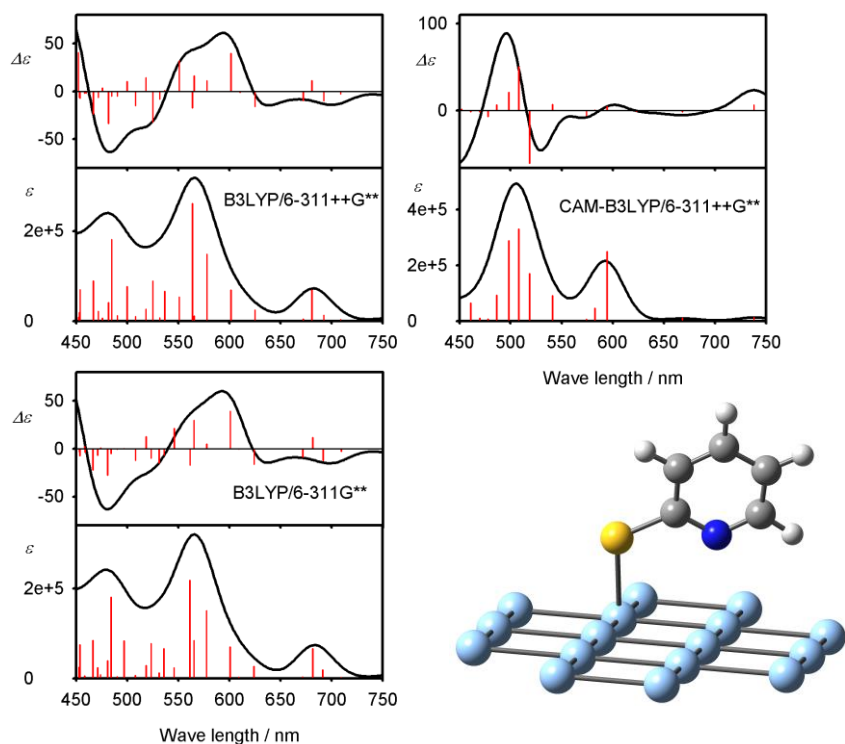
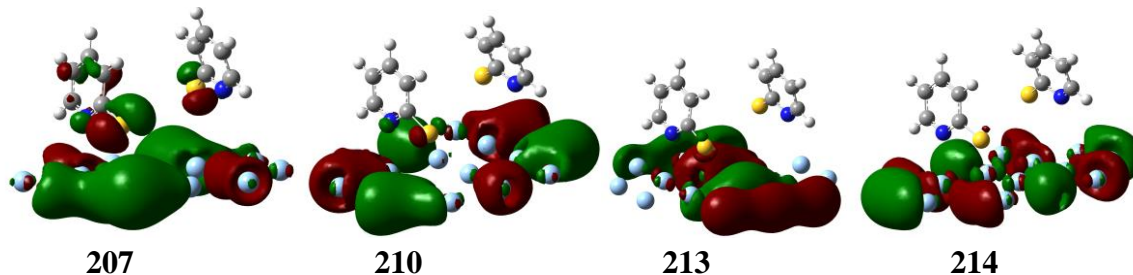


**Figure S8.** CD and absorption spectra of the first model calculated at three approximation levels, always with the CPCM solvent and MWB28 silver effective core potential.

**Table S3.** Cluster 2, transitions within 520-540 nm, and example of involved orbitals

$\lambda / \text{nm}$	$D / \text{debye}^2$	$R / \text{debye}^2$	$R/D \times 10^4$	from <sup>a</sup>	to
545	17	-0.0025	-1.4	210	217
543	48	0.0098	2.0	207	213
534	14	-0.0119	-8.6	207	214
527	64	-0.0056	-0.9	203	211
525	16	-0.0035	-2.2	207	214
518	1	0.0002	2.5	206	212
511	22	-0.0028	-1.3	202	211
501	0	-0.0003	-8.7	210	220

<sup>a</sup> dominant orbital contribution, 210 = HOMO, 211 = LUMO.





## Experimental Details

**Preparation of Borate-Stabilized Silver Nanoparticles.** The synthesis was based on previously described procedures.<sup>2-4</sup> Solution "1" was prepared by mixing 20.5  $\mu\text{L}$  of silver nitrate 0.182 M solution with 3.73 g of water, solution "2" consisted of 11.5  $\mu\text{L}$  2.01 M  $\text{NaBH}_4$  solution and 11.25 g of water. For  $\text{NaBH}_4$ , we used commercial (Sigma-Aldrich, cat. no. 215511) triethylene glycol dimethyl ether solution, avoiding handling hygroscopic solid  $\text{NaBH}_4$  and meta-stable aqueous or methanol solutions also sometimes used.<sup>2,4</sup> Solution 1 was added (one drop per second) to solution 2 under constant stirring, and the stirring continued for another 3 min. Then the mixture was filtered either with cotton plug or membrane filter (0.1  $\mu\text{m}$  pore size, 33 mm diameter, Millex VV syringe). It should be noted that the colloid quality was quite sensitive to preparation conditions; in about 20% of the cases a premature aggregation occurred and the resultant colloid could not be used. The filtrate was left about 12 h at the room temperature, and then stored at 5° C. The best SEROA spectra were obtained after the colloid matured for 7 days after the preparation, and the colloid was then still usable after several months.

**SERS and ROA Spectra.** Immediately before the measurement 60  $\mu\text{L}$  of the colloid solution was mixed with 20  $\mu\text{L}$   $10^{-4}$  M solution of a linker (2-mercaptopyridine, 2-MPY, 4-mercaptopyridine, 4-MPY, 4-mercaptophenol, 4-MPH, or 2-mercaptopyrimidine, 2-MP) and 5  $\mu\text{L}$   $10^{-4}$  M solution of a chiral acid (tartaric acid, alanine, and arginine). 0.5  $\mu\text{L}$  of 1 M HCl was added to initialize the aggregation, which resulted in pH ~ 2.5. For an average colloid radius of 10 nm<sup>4</sup> we estimate that the concentration of the linker was about five-times bigger than needed to completely cover the silver surface; the molar ratio of the linker and analyte molecules was about four. SERS and ROA spectra were collected on a BioTools ChiralRaman-2XTM spectrometer within 90 - 2100  $\text{cm}^{-1}$ , using 532 nm excitation laser wavelength. The laser power was set to 100-150 mW at the beginning of the measurement to optimize SERS signal for each sample. The spectra were accumulated within 1-3 hours. Some experiments were repeated with analogous results on custom-build spectrometer<sup>5-6</sup> in Palacký University, Olomouc. Here the laser power was fixed at 136 mW.

**CD and UV-vis Absorption.** CD spectra were acquired using a J-815 CD spectrometer (Jasco, Japan) equipped with a xenon lamp as the UV/Vis source and a photomultiplier tube (PMT) detector. Temperature was maintained at 20 °C, the samples were kept in 10-mm Quartz Suprasil optical cell (Hellma, Germany), using scanning speed of 50 nm/min, 1 s integration time, and 2 nm resolution. Solvents spectra measured at identical conditions were subtracted using the Spectra Manager software, ver. 2.08.04 (Jasco, Japan). Absorption was calculated based on the PMT

voltage; for the presentation the absorption spectra were re-measured on a PhotoLab 7600 UV-VIS spectrometer.

**Computational Models.** Three clusters consisting of one or two 2-mercaptopyridine ions (2-MPY<sup>-</sup>) and 13/20 silver atoms ([Figure S9](#)) have been used to investigate spectroscopic properties of the linkers chirally arranged on the silver surface. The positions of silver atoms have been kept constant according to the crystal structure,<sup>7</sup> the ions have been optimized by energy minimization. For the cluster number 3, full optimization including the silver atoms was performed as well, which did not significantly alter the results. The B3LYP<sup>8</sup> functional was used with the 6-311G\*\* basis set for 2-mercaptopyridine and MWB28<sup>9</sup> pseudopotential for silver, within the Gaussian<sup>10</sup> program. The environment was included as the conductor-like<sup>11</sup> polarizable solvent model (CPCM).<sup>12</sup> For further tests, the CAM-B3LYP<sup>13</sup> functional and the 6-311++G\*\* basis set were used as well. The absorption and circular dichroism spectra were calculated using the time-dependent density functional theory (TDDFT)<sup>14</sup> at the same level as the geometry. Similarly, pre-resonance Raman and ROA spectra were obtained by Gaussian at the harmonic approximation for several excitation frequencies.<sup>15</sup>

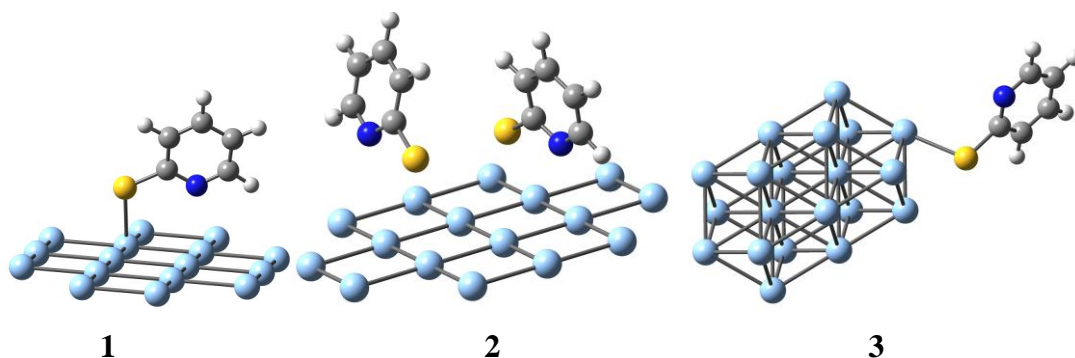


**Figure S9.** Optimized geometries of clusters of one (1) and two (2) 2-mercaptopyridine ions (with -1 charge) attached to 13 silver atoms in plane, and a similar model with one 2-MPY<sup>-</sup> molecule and 20 silver atoms (3).

## References

1. Do, W. H.; Lee, C. J.; Kim, D. Y.; Jung, M. J., Adsorption of 2-mercaptopyridine and 4-mercaptopyridine on a silver surfaces investigated by SERS spectroscopy. *J. Ind. Eng. Chem.* **2012**, *18* (6), 2141-2146.
2. Mulfinger, L.; Solomon, S. D.; Bahadory, M.; Jeyarajasingam, A. V.; Rutkowsky, S. A.; Boritz, C., Synthesis and Study of Silver Nanoparticles. *J. Chem. Educ.* **2007**, *84*, 322–325.
3. Khaydarov, R. A.; Khaydarov, R. R.; Gapurova, O.; Estrin, Y.; Scheper, T., Electrochemical method for the synthesis of silver nanoparticles. *J. Nanopart. Res.* **2009**, *11* (5), 1193-1200.

4. Niederhafner, P.; Šafařík, M.; Neburková, J.; Keiderling, T. A.; Bouř, P.; Šebestík, J., Monitoring peptide tyrosine nitration by spectroscopic methods. *Amino Acids* **2020**, <https://doi.org/10.1007/s00726-020-02911-7>.
5. Michal, P.; Čelechovský, R.; Dudka, M.; Kapitán, J.; Vůjtek, M.; Berešová, M.; Šebestík, J.; Thangavel, K.; Bouř, P., Vibrational Optical Activity of Intermolecular, Overtone, and Combination Bands: 2-Chloropropionitrile and  $\alpha$ -Pinene. *J. Phys. Chem. B* **2019**, *123* (9), 2147-2156.
6. Palivec, V.; Michal, P.; Kapitán, J.; Martinez-Seara, H.; Bouř, P., Raman Optical Activity of Glucose and Sorbose in Extended Wavenumber Range. *ChemPhysChem* **2020**, *21* (12), 1272-1279.
7. Spreadborough, J.; Christian, J. W., High-temperature X-ray diffractometer. *J. Sci. Instrum.* **1959**, *36*, 116-118.
8. Becke, A. D., Density-functional thermochemistry. III. The role of exact exchange. *J. Chem. Phys.* **1993**, *98*, 5648-5652.
9. Figgen, D.; Rauhut, G.; Dolg, M.; Stoll, H., Energy-consistent pseudopotentials for group 11 and 12 atoms: adjustment to multi-configuration Dirac-Hartree-Fock data. *Chem. Phys.* **2005**, *311* (1), 227-244.
10. Frisch, M. J.; Trucks, G. W.; Schlegel, H. B.; Scuseria, G. E.; Robb, M. A.; Cheeseman, J. R.; Scalmani, G.; Barone, V.; Petersson, G. A.; Nakatsuji, H.; Li, X.; Caricato, M.; Marenich, A. V.; Bloino, J.; Janesko, B. G.; Gomperts, R.; Mennucci, B.; Hratchian, H. P.; Ortiz, J. V.; Izmaylov, A. F.; Sonnenberg, J. L.; Williams-Young, D.; Ding, F.; Lipparini, F.; Egidi, F.; Goings, J.; Peng, B.; Petrone, A.; Henderson, T.; Ranasinghe, D.; Zakrzewski, V. G.; Gao, J.; Rega, N.; Zheng, G.; Liang, W.; Hada, M.; Ehara, M.; Toyota, K.; Fukuda, R.; Hasegawa, J.; Ishida, M.; Nakajima, T.; Honda, Y.; Kitao, O.; Nakai, H.; Vreven, T.; Throssell, K.; Montgomery Jr., J. A.; Peralta, J. E.; Ogliaro, F.; Bearpark, M. J.; Heyd, J. J.; Brothers, E. N.; Kudin, K. N.; Staroverov, V. N.; Keith, T. A.; Kobayashi, R.; Normand, J.; Raghavachari, K.; Rendell, A. P.; Burant, J. C.; Iyengar, S. S.; Tomasi, J.; Cossi, M.; Millam, J. M.; Klene, M.; Adamo, C.; Cammi, R.; Ochterski, J. W.; Martin, R. L.; Morokuma, K.; Farkas, O.; Foresman, J. B.; Fox, D. J. *Gaussian 16 Rev. A.03*, Gaussian, Inc.: Wallingford, CT, 2016.
11. Klamt, A., COSMO and COSMO-RS. In *The Encyclopedia of Computational Chemistry*, Schleyer, P. R.; Allinger, N. L.; Clark, T.; Gasteiger, J.; Kollman, P. A.; Schaefer III, H. F.; Schreiner, P. R., Eds. John Wiley & Sons: Chichester, 1998; Vol. 1, pp 604-615.
12. Cossi, M.; Rega, N.; Scalmani, G.; Barone, V., Energies, Structures, and Electronic Properties of Molecules in Solution with the C-PCM Solvation Model. *J. Comput. Chem.* **2003**, *24* (6), 669-681.
13. Yanai, T.; Tew, D.; Handy, N. C., A new hybrid exchange-correlation functional using the Coulomb-attenuating method (CAM-B3LYP). *Chem. Phys. Lett.* **2004**, *393*, 51-57.

14. Furche, F.; Ahlrichs, R., Adiabatic time-dependent density functional methods for excited state properties *J. Chem. Phys.* **2002**, *117* (6), 7433-7447.
15. Cheeseman, J. R.; Frisch, M. J., Basis Set Dependence of Vibrational Raman and Raman Optical Activity Intensities. *J. Chem. Theory Comput.* **2011**, *7* (10), 3323-3334.